DMD Fast Forward. Published on September 22, 2008 as doi:10.1124/dmd.108.020750

DMD #20750

Design, data analysis and simulation of *in vitro* drug transport kinetic experiments using a mechanistic *in vitro* model

Agnès Poirier, Thierry Lavé, Renée Portmann, Marie-Elise Brun, Frank Senner, Manfred Kansy, Hans-Peter Grimm and Christoph Funk

F. Hoffmann-La Roche Ltd. ; Non-Clinical Development; Drug Safety; Basel, Switzerland

Running title: Design, data analysis and simulation of transport kinetics

Corresponding author: Dr. Christoph Funk

F. Hoffmann La Roche A.G.

Non-Clinical Drug Safety, 69/154

Grenzacherstrasse 124

4070 BASEL – SWITZERLAND

E-mail: christoph.funk@roche.com

Tel: +41 (0)61 688 2308

Fax : +41 (0)61 688 2908

Text pages: 32

Tables: 1

Figures: 7

References: 45

Words in abstract: 259

Words in introduction: 813

Words in discussion: 1666

Abbreviations: OATP, organic anion transporting peptide; P_{dif}, passive diffusion; V_{max}, Michaelis-Menten maximum transport rate; K_m, Michaelis-Menten affinity constant; $C_{intracell}$, intracellular concentration; $U_{intracell}$, total protein quantity per well in mg; $B_{intracell}$, intracellular quantity per mg of protein in pmol/mg; $V_{intracell}$, intracellular volume per well in µl; $A_{intracell}$, intracellular quantity per well in pmol; C_{me}, incubation medium concentration; V_{me}, incubation medium volume; v_0, initial uptake rate; f_b, fraction of drug non-specificly bound; PBPK, physiologically based pharmacokinetic; CCK8, cholecystokinin octapeptide sulphated; CHO cells, chinese hamster ovary cells; CV, coefficient of variation.

Abstract

The use of *in vitro* data for quantitative predictions of transporter-mediated elimination *in vivo* requires an accurate estimation of the transporter Michaelis-Menten parameters, V_{max} and K_m, as a first step. Therefore, the experimental conditions of *in vitro* studies used to assess hepatic uptake transport were optimized regarding active transport processes, non-specific binding and passive diffusion (P_{dif}). A mechanistic model was developed to analyse and accurately describe these active and passive processes. This two-compartmental model was parameterized to account for non-specific binding, bidirectional passive diffusion, and active uptake processes based on the physiology of the cells. The model was used to estimate kinetic parameters of *in vitro* transport data from organic anion transporting peptide (OATP) model substrates (e.g. CCK8, deltorphin II, fexofenadine, pitavastatin). Data analysis by this mechanistic model significantly improved the accuracy and precision in all derived parameters (mean coefficient of variation for V_{max} and K_m were respectively 19% and 23%) as compared to the conventional kinetic method of transport data analysis (mean CV% were respectively 58% and 115% using this method). Furthermore, permeability was found to be highly temperature-dependent in CHO control cells and artificial membranes (PAMPA). While for some compounds (taurocholate, estrone-3-sulfate, propranolol) the effect was moderate (1.5 to 6-fold higher permeability at 37°C compared to 4°C), for fexofenadine a 16 fold higher passive permeability was seen at 37°C. Therefore, P_{dif} was better predicted if evaluated under the same experimental conditions as V_{max} and K_m, i.e. in a single incubation of CHO over-expressed cells or rat hepatocytes at 37°C, instead of a parallel control evaluation at 4°C.

Introduction

Increasing importance has been given in the last years to active drug transport processes in pharmacokinetics (Chandra and Brouwer, 2004; Shitara et al., 2006). In addition to metabolism, elimination of drugs can be strongly dependent on hepatic and/or renal transport processes and drug-drug interactions can be transporter-related as well (Petzinger-Ernst, 2006; Poirier et al., 2007). In the liver, the interplay between uptake and export processes influences the drug intracellular concentration and thereby the amount of drug available for metabolic elimination and/or biliary excretion. Therefore, hepatic uptake of new chemical entities is increasingly studied in pre-clinical development.

Primary hepatocytes, plated or in suspension, as well as cell lines over-expressing individual transporters, are widely used to assess active hepatic uptake processes (Komai et al., 1992; Ismair et al., 2001; Shitara et al., 2003; Ho et al., 2006; Poirier et al., 2007). Nevertheless these cellular systems represent only one component of the dynamic and interlinked processes occurring in liver tissue. Therefore it remains a major challenge to predict quantitatively hepatic transport processes based on *in vitro* data (Bentz et al., 2005; Hallifax and Houston, 2006; Liu and Pang, 2006; Ekins et al., 2007; Webborn et al., 2007). Additional processes, such as non-specific binding and bidirectional passive diffusion between medium and cells need to be assessed separately from active transport in order to enable proper mechanistic scaling. In particular for lipophilic compounds, extensive adsorption to cells and culture materials is often observed (Ishiguro et al., 2006).

In hepatocytes, passive processes are typically assessed in a parallel incubation at 4ºC to disable any active transport proteins (Komai et al., 1992; Ismair et al., 2001; Shimada et al., 2003; Lancon et al., 2004; Treiber et al., 2004; Ho et al., 2006). However, while active transport is inhibited at low temperature, passive processes might also be altered as membrane fluidity decreases (Frezard and Garnier-Suillerot, 1998; Neuhoff et al., 2005; Webborn et al.,

2007). Nevertheless these limitations in the control incubations performed at low temperature have not been addressed systematically in uptake experiments up to now. Alternatively, active transport processes might be inhibited by specific inhibitors to assess the remaining passive processes. However, such selective inhibitors are not yet available for many of the transporters relevant in drug distribution and elimination (Hirano et al., 2006; Webborn et al., 2007). In addition they might also influence multiple other processes in the cell systems used (Boelsterli et al., 1988; Ratanasavanh et al., 1996). Optionally, passive processes can be assessed by including in the experiment high concentrations where active transport processes are saturated allowing the determination of passive diffusion processes (Hirano et al., 2004; Yamashiro et al., 2006). The high substrate concentrations used in this approach might however lead to a deviation from a linear uptake rate, in particular for highly lipophilic compounds (Baker and Parton, 2007; Parker and Houston, 2008)(Fig5). Therefore, the typically performed single incubation time points are not appropriate and linear conditions, resulting in true initial transport rates, can not be assumed. Mechanistic approaches to analyze *in vitro* transport data have hence been discussed recently (Gonzalez-Alvarez et al., 2005; Baker and Parton, 2007).

Kinetic parameters of drug transporters are usually assessed in a stepwise procedure. Initial uptake rates are determined based on a single incubation time point for multiple concentrations, followed by a determination of the basic Michaelis-Menten parameters (K_m and V_{max}) in a second step (Komai et al., 1992; Ismair et al., 2001; Treiber et al., 2007). However, initial rates based on multiple measured time points are rarely established, although an important prerequisite of Michaelis-Menten kinetics. And for many compounds the assumption of linear initial transport rates might be violated in the presence of the bidirectional passive diffusion, the non-specific binding, and the decrease in extracellular concentration. In the proposed mechanistic model, using multiple time points determined *in*

vitro, such time-dependent non-linearities can be described and the underlying processes can be better quantified.

In the present study, the experimental setup for *in vitro* assays was optimized with respect to both active and passive processes. Taurocholate, estrone-3-sulfate, CCK8, deltorphin II, fexofenadine, napsagatran, pravastatin, pitavastatin and fluvastatin were chosen as well-known substrates of multiple uptake transporters (van Montfoort et al., 2003; Kopplow et al., 2005). In addition two proprietary compounds and propranolol, as a highly permeable compound, were included to cover a broad range of physicochemical parameters. A mechanistic mathematical model addressing the time-dependent changes in compound concentrations and the underlying passive (P_{dif}) and active processes was developed. It allowed a standardized assessment of *in vitro* transport data to derive V_{max}, K_m, P_{dif} and non-specific binding values. The robustness of the approach was tested using both, experimental data from *in vitro* transport experiments and theoretical transport data. The improved experimental conditions in conjunction with the mechanistic model for data evaluation were found to deliver transport kinetic data of greatly improved quality, a prerequisite for subsequent extrapolation to *in vivo* using PBPK models.

Materials and Methods

Materials.

[^{3}H]-fexofenadine and [^{3}H]-pravastatin were obtained from Moravek Biochemicals (Brea, CA), [^{3}H]-[D-Ala2]-deltorphin II, [^{3}H]-taurocholic acid, [^{3}H]-propranolol and [^{3}H]-estrone-3-sulfate were from Perkin Elmer (Boston, MA), [^{3}H]- pitavastatin calcium was from ARC (St Louis, MO), [^{3}H]-cholecystokinin octapeptide sulphated ([^{3}H]-CCK8) was from GE Healthcare (UK). Pravastatin and pitavastatin calcium was obtained from APIN Chemicals LTD (UK), [D-Ala2]-deltorphin II and cholecystokinin octapeptide sulphated (CCK8) were from Bachem (Bubendorf, Switzerland), propranolol, fexofenadine, estrone-3-sulfate and taurocholic acid were from Sigma (Buchs, Switzerland). [^{14}C]-napsagatran and napsagatran were produced in house (structure in Ries and Wienen, 2003). All cell culture media and reagents were purchased from Invitrogen Corporation (Paisley, UK) and standard tissue culture flasks and 24-well plates were from Falcon/Becton Dickinson (Franklin lakes, NJ).

PAMPA experiments.

As previously described (Fischer et al., 2007), for PAMPA assay, a “sandwich” was formed from a 96-well filter plate and a 96 well in-house made Teflon plate, such that each well is divided into two chambers: donor at the bottom and acceptor at the top, separated by microfilter with a pore size of 0.45µm polyvinylidene fluoride (PVDF) from Millipore (Billerica, MA), coated with a 10% (w/v) egg phosphatidylcholine and 0.5% (w/v) cholesterol dissolved in dodecane. Compounds were introduced as 10mM DMSO stock solutions in a 96-well microtitre plate. An automated liquid handling system draws an aliquot of the DMSO and mixes it into a buffer solution (0.05M MOPSO with 0.5% (w/v) glycocholic acid at pH 6.5), so that the final sample concentration is 150µM and the DMSO concentration is 1.5% (v/v). A part of the sample solutions was filtered, using a 96-well PVDF filter plate from

Corning (Corning, NY), and added to the donor compartments. In the acceptor compartment the same buffer system at the same pH is used than in the donor compartment but devoid of glycocholic acid. After 18h incubation at 4°C or 37°C, the sandwich plates were separated and both the donor and acceptor compartments were measured for the amount of material present, by comparison with the UV spectra (250–500 nm) obtained from reference standards. All measurements were done in triplicate. Effective permeability values (Pe) were calculated as described by (Avdeef et al., 2001; Fischer et al., 2007). The PAMPA Evolution Software v3.3 from pION Inc. (Woburn, MA) was used for all Pe calculations.

OATP expressing cell-lines.

CHO cells (Chinese hamster ovary cells) overexpressing Oatp1a1 or OATP1B1 were transfected respectively with pTriEx-3 Neo-Oatp1a1 or OATP1B1 construct as described previously (Noe et al., 2007). Single clones were selected based on functional activity and characterized. The CHO cells overexpressing Oatp1b2 and OATP1B3 were obtained from the lab of Peter Meier-Abt, University of Zürich, Switzerland. Culturing of the cells was performed as described previously (Noe et al., 2007). CHO cells were grown in HAM's F-12K medium, 2.5 g/L sodium bicarbonate, supplemented with 10% FCS, penicillin-streptomycin solution, plus geneticin (0.5 mg/ml) for CHO-Oatp1a1, CHO-OATP1B1 and CHO-OATP1B3, or hygromycin (0.5 mg/ml) for CHO-Oatp1b2 cells. Cells were cultivated at 37ºC in a humidified 5% CO_2 cell culture incubator. For transport assay, cells were split as follows: cells from a confluent 75 cm^2 flask (detached with trypsin-EDTA) were uniformly re-suspended in the desired volume of HAM's F-12K medium. 1 ml of the uniformly re-suspended cells (2.10^5 cells / ml) were added to each well of a 24-well plate. The cells were used for transport assays 38 to 42 hours later, when they were 80-90% confluent.

Preparation and plating of primary rat hepatocytes.

Isolation and conventional primary culture of rat hepatocytes were performed as described previously (Luttringer et al., 2002; Blanchard et al., 2004). Hepatocytes were isolated from adult male Wistar rat (~250 g) liver by a previously described two-step collagenase perfusion method (Seglen, 1979; Luttringer et al., 2002). Cell viability was determined from exclusion of erythrosine-B by the cell membranes. Only the cell preparations that exhibit a viability over 80% were retained for further studies. Freshly prepared hepatocytes were seeded at $4 \cdot 10^5$ cells/well on precoated 24-well plates (Becton Dickinson BioCoat™ Collagen I). Cells were cultured for 3 hours in a humidified chamber maintained at 37°C, 5% CO_2 in attachment medium composed of Williams' E medium supplemented with 10% fetal calf serum, 0.5% streptomycin/penicillin, insulin (1.2 µM) and glutamine (400 µM).

***In vitro* uptake experiments.**

Recombinant cells or hepatocytes were prepared as outlined above and the uptake assays were performed as described previously with minor modifications (Noe et al., 2007). Assays were run using two or three wells as one set. The medium was removed from the wells by aspiration. The wells were washed once with 1 ml of HBSS (Hank's balanced salt solution (InVitrogen/GIBCO) for cell lines or HBSS containing calcium and magnesium for hepatocytes) at 37°C. The uptake experiment was started by aspiration of wash buffer and adding 150 µl of a pre-warmed 37°C (or ice-cold for 4°C incubation) HBSS solution containing the substrate of interest. The plate was transferred on a 37°C heating block (Eppendorf) (or on ice for 4°C incubation). After the incubation time, the plate was removed from the heating block and immediately 1 ml ice-cold PBS containing 0.2% bovine serum albumin (BSA) was added to stop the transport activity with the ice cold buffer and the large volume of PBS effectively diluting the compound (stop step). The solution was removed by

aspiration. BSA was also included in the subsequent washing buffer to minimize background due to non-specific binding of radiolabelled compound. The following washing steps were performed rapidly with warmed (37°C) or ice cold (4°C) buffer as indicated in the respective experiments. The cells were washed twice with PBS containing 0.2% BSA, with 2 ml each (first and second wash steps) and once with PBS without BSA (3 ml) to remove added BSA protein (third wash step). Then 0.5 ml of 1% TritonX were added to solubilize the cells. After incubation for 15 min on a heated shaker at 60°C, 0.25 ml of the solubilized cell mix was added to 4 ml of scintillation fluid and radioactivity was determined by liquid scintillation counting. Protein content was determined for each well using the Pierce BCA assay (Pierce, Rockford, IL, USA) with BSA as standard according to the manufacturers' protocol.

Kinetic *in vitro* experiment.

Kinetic experiments were carried out as described above on 24-well plates. One experiment consisted of the drug of interest incubated at 6 to 8 different concentrations which were adjusted after a first experiment to cover K_m and P_{dif} evaluation. Three different time points were used per drug concentration (usually 30s – 60s – 90s) and each time point was done in duplicate. Kinetic parameters were calculated from three independent experiments using either different batches of cells or hepatocytes prepared from 3 different rats.

Data analysis of kinetic experiments and mechanistic model.

The cellular uptake process consists in both an active, saturable process and a passive component. The active transport can be characterized by Michaelis-Menten parameters (V_{max}, K_m), while the passive process is represented by the passive diffusion P_{dif}. Two different methods, the conventional two-step approach and a mechanistic model were compared for the estimation of V_{max}, K_m, and P_{dif}.

Conventional two-step approach

The kinetic analysis of experimental data consisted of two consecutive steps. In the first step, measured compound accumulation in cell reported to mg of protein ($B_{intracell}$ in pmol/mg) was plotted against time for each incubation medium concentration (C_{me} in µM, nominal values). This intra-cellular accumulation was assumed to be the sum of an initial binding α and a linear increase with time at a constant rate v_0. The following equation was used to fit α and v_0 for each C_{me} tested:

$$B_{intracell}(t) = \alpha + v_0 * t \qquad \text{Equation 1}$$

In this first step, duplicates for each of the three time points were fitted, corresponding to 6 data points per concentration. In the second step, initial uptake rates were plotted against medium concentrations and V_{max}, K_m, and P_{dif} were fitted according to Equation 2. It was assumed in this model that the initial uptake rate (v_0) is a function of the medium concentration, with contributions of active uptake (Michaelis-Menten) and passive unidirectional diffusion (from medium into cells). The number of points available for fitting in the second step was depending on the number of medium concentrations tested (6 to 8).

$$v_0(C_{me}) = \frac{V_{max} * C_{me}}{K_m + C_{me}} + P_{dif} * C_{me} \qquad \text{Equation 2}$$

V_{max} was expressed in pmol/min/mg, K_m in µM, and P_{dif} in µl/min/mg.

Mechanistic model

The *in vitro* assay was described by two compartments corresponding to the incubation medium for one well (volume V_{me}, nominal value of compound concentration C_{me} in µM) and intracellular space of all cells in one well (volume $V_{intracell}$, quantity of compound in one well $A_{intracell}$ in pmol and compound concentration in µM $C_{intracell} = \frac{A_{intracell}}{V_{intracell}}$) as depicted in Figure

1. The volume V_{me} was 150 µl. For the determination of $V_{intracell}$ (in µl), the total quantity of protein per well ($U_{intracell}$ in mg) was converted to number of cells by applying an experimentally determined constant of 1 mg protein per million rat hepatocytes (1.06 ± 0.18 mg/10^6cells, n=5, equal to (Shitara et al., 2004)) or 0.15 mg per million CHO cells (0.152 ± 0.032 mg/10^6cells, n=11). A cell volume of 3.9 µl per million hepatocytes (Reinoso et al., 2001) or 1.40 µl per million CHO cells (mean of two publications: 1.28 µl (Sarkadi et al., 1984) and 1.53 µl (Vickers et al., 1993)) was then applied to calculate the intracellular volume in µl in one well ($V_{intracell}$).

The time-course of the quantity of compound in the intracellular compartment was modeled by the following differential equation:

$$\frac{dA_{intracell}}{dt} = \frac{V_{max} * C_{me}}{K_m + C_{me}} + P_{dif} * C_{me} - P_{dif} * C_{intracell} \qquad \text{Equation 3}$$

In equation 3 bi-directionality of passive diffusion was included by the introduction of the last, time-dependent, term in this equation ($-P_{dif} * C_{intracell}$). In control cells (ie CHOneo cells incubated at 4ºC or 37ºC or rat hepatocytes incubated at 4ºC) the active uptake process was omitted and the following equation was used to estimate P_{dif}:

$$\frac{dA_{intracell}}{dt} = P_{dif} * C_{me} - P_{dif} * C_{intracell} \qquad \text{Equation 4}$$

In equation 3 and 4, V_{max} was expressed in pmol/min, K_m in µM, and P_{dif} in µl/min and were calculated parameters for one well equivalent. So, $U_{intracell}$ being the total amount of protein in one well (mg), the obtained V_{max} and P_{dif} in equation 3 and 4 needed to be converted as follow:

$$P_{dif}\ (\mu l/\text{min/mg}) = \frac{P_{dif}\ (\mu l/\text{min})}{U_{intracell}\ (\text{mg})} \qquad V_{max}\ (\text{pmol/min/mg}) = \frac{V_{max}\ (\text{pmol/min})}{U_{intracell}\ (\text{mg})}$$

A non-zero initial condition for the intracellular amount was used for equations 3 and 4 to account for non-specific binding (to cells and/or experimental supports). The amount of

initially bound compound was assumed to be proportional to C_{me} and $V_{intracell}$ with the constant f_b being the bound fraction.

$$A_{intracell}(t=0) = f_b * C_{me} * V_{intracell} \qquad \text{Equation 5}$$

This mechanistic *in vitro* model was implemented in ModelMaker v.4® (Cherwell Scientific Ldt., UK). Numerical integration was performed using the Runge-Kutta method. The Marquardt optimization algorithm was used to simultaneously estimate the parameters f_b, V_{max}, P_{dif} and K_m. In a typical kinetic experiment, using this method, all data points were fitted in a single step using equation 3, duplicates for each of the three time points for each concentration, resulting in 36 to 48 data points.

Computer generation of virtual data sets

To cover extended compound properties, height different scenarios of P_{dif}, non-specific binding, V_{max} and K_m were generated, each of them consisting of six sets of data. One data set consisted of 7 concentrations (C_{me}) (0.3-300µM) with 3 time points each (30s, 60s, 90s), and duplicate $C_{intracell}$ per time point, corresponding to one virtual experiment (42 $C_{intracell}$ or 42 virtual wells). The datasets were generated – using the random number generation function of Excel® – through random sampling assuming normal distribution with a standard deviation of 10% and solving equation 3 to generate the intracellular concentration as a function of time. Each set of data was then analyzed with both, the conventional two-step approach and the mechanistic model.

Statistical evaluation of data

Standard deviations were calculated for all parameters obtained from the individual experiments. Triplicate experiments were run and mean values were calculated for all

parameters. The standard deviations were propagated following the rules of propagation of errors (Lindberg, 1997) to account for the uncertainty due to the measurement.

To compare the mean P_{dif} calculated in different experimental conditions, Student's t-test was used to test the equality of the means. To compare the accuracy of the two different approaches of kinetic analysis, Student's t-test was used to test the equality of the coefficient of variation in each population. To compare the ability of evaluating an identical K_m for selective substrates, Student's t-test was used to test the equality of the K_m in CHO-Oatp1b2 cells and rat hepatocytes for CCK8 and deltorphin II for each data analysis method separately. For all tests, the null hypothesis was rejected for a p-value smaller or equal to 0.05.

Results

Reduction of non-specific binding to cells and cell culture plates.

Typically, much less than 0.1% of the radiolabeled substrate supplied in the incubation medium enters the cells. Efficient washing of excess substrate is therefore of particular importance when cell-associated compound is assessed. In initial experiments, high non-specific binding was observed to cells, culture plates and to the collagen layer in the case of hepatocytes. This non-specific binding was compound- and temperature-dependent and therefore difficult to control, in particular for highly lipophilic compounds incubated with hepatocytes.

In order to reduce non-specific binding to cell culture plates, binding of deltorphin II, CCK8, taurocholic acid and pravastatin to collagen-coated and non-coated plates was assessed using different washing temperatures. These empty plates were treated equally to plates with cells. A significant decrease in non-specific bound radioactivity was observed for all substrates tested (67±12% mean decrease) if washing of the plate was performed at 37°C instead of at 4°C.

A similar effect was seen for plates containing cells. Although the last wash step was virtually devoid of radioactivity (0.02 to 0.09%) suggesting an efficient washing of non-specifically bound radioactivity, the overall recovery of radioactivity could be improved from 80-96% at 4°C to 85-100% at 37°C. This increased efficiency of washing at 37°C was seen particularly if high drug concentrations were tested.

In order to ensure that the reduced residual cellular substrate levels were not due to increased cell leakage at 37°C, the first wash step was extended over 7 minutes to follow radioactive substrate leakage over this prolonged time interval. A comparable leakage was observed irrespective of the temperature for several compounds and cell lines – including rat hepatocytes. The example of deltorphin II in CHOneo (control) and CHO-Oatp1b2 cells is

shown in Figure 2. Comparing the extended washings at 4°C and 37°C an equivalent slope, and hence leakage, was seen irrespective of the washing temperature. The initial difference in cell-associated compound is considered to be due to an improved efficiency of the washing at 37°C. By keeping each wash step as short as possible in routine assays, the leakage can be minimized and the non-specific binding reduced by the washing at 37°C.

Evaluation of passive diffusion (P_{dif}) in cell lines and hepatocytes.

The passive diffusion was assessed at 37°C and 4°C using an artificial phospholipid membrane (PAMPA), different cell lines and hepatocytes for five transporter substrates plus propranolol as a high passive permeability compound. A significant temperature dependent difference in drug uptake was observed in PAMPA and CHOneo cells, believed not to express any drug transport activity (Figure 3). For all compounds a linear, concentration-dependent increase of cell-associated compound was observed in CHOneo cells, without indication of any saturable process. The passive diffusion of these compounds in the cellular system resulted in a comparable ranking to the one obtained based on measured permeabilities for artificial membranes (Pe from PAMPA), supporting that mainly passive diffusion was observed in those CHOneo cells. A statistically significant underestimation of both P_{dif} and Pe was observed when CHOneo cells and artificial membranes were incubated at 4ºC instead of 37ºC (Figure 3). The temperature-dependent effects were particularly high for fluvastatin and fexofenadine with 7.6 and 16-fold decreased apparent “uptake” in the 4°C control incubation of CHOneo cells. On the other hand, the smallest temperature effects were observed for compounds with extreme permeability values, either low (estrone-3-sulfate and taurocholate) or very high (propranolol).

The passive diffusion of three Oatp transporter substrates was evaluated using CHO control cells and the same cells over-expressing either Oatp1a1 or Oatp1b2 transporter. Kinetics were

determined at 37°C in triplicate for each compound and the passive diffusions were evaluated using either equation 3 for the Oatp over-expressing cells or equation 4 for the CHO control cells (Figure 4A). Low passive diffusion was observed for deltorphin II and CCK8 (all < 0.1 µl/min/mg), while fexofenadine had a higher passive diffusion of around 7 µl/min/mg. For each compound, a comparable passive diffusion could be observed, in CHO-Oatp expressed cells using equation 3 which includes active and passive transport, and in CHOneo cells using equation 4 which includes only passive transport. These results support the assumption that CHOneo cells do not express significant transport protein and can therefore be used to study passive diffusion. Since for hepatocytes the typical negative control in transport studies is a parallel incubation at 4°C, the passive diffusion was compared under these conditions for the same three Oatp substrates (Figure 4B). A statically higher P_{dif} was observed for the 37°C incubations for all compounds. Deltorphin II and CCK8 showed low absolute values of P_{dif} (<1 µl/min/mg), and negligible P_{dif} relative to the active uptake into the cell. However for fexofenadine, which showed a higher absolute P_{dif} (~2 µl/min/mg at 37°C), the estimated parameter from the 4ºC incubation was about three times lower than the value obtained at 37°C (Figure 4B).

Analysis of kinetic experiments and testing of mechanistic model.

A mechanistic model addressing the different interrelated and time-dependent processes of active uptake, non-specific binding and passive diffusion was used to evaluate *in vitro* transport data as described in Materials and Methods. The validity of the model and the sensitivity of individual parameters were tested by analyzing different real and virtual data sets.

Sensitivity analysis

DMD Fast Forward. Published on September 22, 2008 as DOI: 10.1124/dmd.108.020750
This article has not been copyedited and formatted. The final version may differ from this version.

A sensitivity analysis was performed to investigate the impact of P_{dif}, K_m and V_{max} on the cellular uptake parameters evaluated using the mechanistic model. Thus, the model was tested for ranges of values typically observed in *in vitro* experiments: P_{dif} was varied from 0 to 70 µl/min/mg, K_m from 1 to 1000 µM, V_{max} from 10 to 3000 pmol/min/mg (Figure 5). For low to medium P_{dif} values (i.e. up to 15 µl/min/mg), the intracellular concentration was strongly influenced by active transport. At low extracellular medium concentrations, K_m had a major impact (Figure 5A), while V_{max} was more important at high extracellular medium concentrations (Figure 5C). On the other hand, for higher P_{dif} values (> 15 µl/mg/min e.g. very lipophilic), the impact of active transport is very unlikely to be detectable even if it contributes significantly to the overall transport into the cell, as the assay sensitivity would be insufficient to detect the correct K_m and V_{max} (Figure 5B and D). In consequence, with a high P_{dif}, Michaelis-Menten parameters would not be accurately estimated, independently of their value. Overall the model behaved as expected and showed that a broad concentration range is required to accurately estimate P_{dif}, K_m and V_{max} within a single experiment, and preferably needs to be determined in a pilot experiment.

The impact of the hepatocyte volume – which is used to calculate the intracellular volume per well ($V_{intracell}$) in µl – on the estimation of the uptake parameters was further investigated. The hepatocyte volume values reported in the literature range from 2.19 to 6.54 µl per 10^6 hepatocytes (Brosnan and Qian, 1994; Reinoso et al., 2001; Baker and Parton, 2007). Interestingly, P_{dif}, V_{max} and K_m remained constant over this range of values. In the present work, an intermediate volume of 3.9 µl per million cells was used (Reinoso et al., 2001). The impact of the accuracy of $V_{intracell}$, which is calculated based on the measured protein level per well, was also assessed. K_m stayed very stable over a wide range of $V_{intracell}$ values (0.04 µl – 12 µl), while P_{dif} and V_{max} increased with increasing $V_{intracell}$. Therefore protein levels should

be measured for each experiment (mean values per plate can be used) to calculate the respective $V_{intracell}$ by applying the scaling factors as outlined.

Data analysis of computer generated set of data

Data for eight virtual compounds covering a wide range of active and passive transport properties and different non-specific binding was generated on the computer. These numerically generated data were then analyzed utilizing both the conventional stepwise approach and the mechanistic model. The results are summarized in Figure 6. Significant differences were seen in the estimation of P_{dif}, V_{max} and K_m between the two approaches. As this comparison was done with a virtual set of data, the estimated parameters could be directly compared to the initially selected values. The parameters estimated from the mechanistic model were always closer to the expected values. Furthermore, the mechanistic model resulted in statistically better precision than the conventional approach. The two methods gave similar results when P_{dif} was negligible, although both accuracy and precision were superior with the mechanistic model. For compound 3, with low passive diffusion (P_{dif}=0.01 µl/min/mg, K_m=32 µM), the mechanistic model yielded a K_m of 31.5±2.9 µM while the two-step approach yielded 26.8±7.5 µM. For a high P_{dif} compound (compound 4, P_{dif} = 14 µl/mg/min, V_{max}=550 pmol/min/mg) V_{max} was estimated at 546±86 pmol/min/mg by the mechanistic model, whereas the two-step approach gave a V_{max} of 109±1580 pmol/min/mg. No significant difference could be observed when changing the incubation time points indicating the robustness of the approach based on the underlying mechanistic assumptions.

Analysis of data from *in vitro* transport experiments

In vitro uptake data were generated for the selected uptake transporter substrates CCK8, fexofenadine, pitavastatin, deltorphin II, napsagatran and proprietary compound B using

either primary rat hepatocytes, rat Oatp1b2, Oatp1a1, human OATP1B1, or OATP1B3 overexpressing cells. The kinetic studies were done under the optimized experimental conditions in triplicate as detailed in Material and Methods. The data were analyzed using both, the step-wise conventional approach and the mechanistic model to determine P_{dif}, K_m and V_{max}. Experimental data from one experiment each are shown in Figure 7 with the respective fitting using the mechanistic model, and all mean parameters are summarized in Table 1. Pitavastatin (Figure 7H) showed low P_{dif} (0.909±1.043 µl/min/mg) and a fraction bound of 0.21±0.10. Much lower affinity and intracellular concentrations and a negligible P_{dif} were measured for CCK8 in CHO cells (Figure 7B and 7C). For compound B, a high P_{dif} (22±10 µl/min/mg) was found. This compound contains a carbonic acid moiety, has a clogP of 4.9 and showed extensive distribution to liver tissue in rats. The high lipophilicity is likely responsible in part for these properties. It showed a rapid deviation from linearity of cellular uptake (data not shown) and the relatively high uncertainty in the estimated kinetic parameters (K_m=373±137 µM, V_{max}=28000±9300 pmol/min/mg, f_b=0.15±0.47 in single pilot experiment) indicated limitations in the approach for such compounds.

Analysis of the experimental *in vitro* data by the two approaches allowed comparison of the resulting K_m values between expressed systems and rat hepatocytes for the two Oatp1b2-selective substrates, CCK8 and deltorphin II for which it should be identical (Table 1). Student's t-test showed a statistically different K_m for CCK8 with the two-step approach, while with the mechanistic model it was identical between CHO-oatp1b2 and rat hepatocytes. For deltorphin II the K_m values were similar using the mechanistic model, while with the conventional approach they were spread apart, although statistically not significantly different due to high variance. Fexofenadine transport data from rat Oatp1a1 expressing cells can not be compared directly to hepatocyte transport data, as rat Oatp1a4 is also involved in fexofenadine transport (Cvetkovic et al., 1999). In addition, specific scaling factors,

compensating for differences in transporter expression levels, have to be established to make a quantitative comparison of transport rates across these experimental systems. For all compounds the accuracy of both methods was assessed by comparing the coefficient of variation (CV) of the estimated parameters. Significant differences were seen in the accuracy of the estimation of V_{max} and K_m for which the mean CV% on the estimates were 19% and 23% with the mechanistic model, and 58% and 115% with the stepwise approach. The individual CV on the P_{dif} parameter estimates were extreme and different between the two methods, however they were spread across a too large range of values to show a statistically significant difference. For example, in the case of CCK8 and deltorphin II, two compounds with a very low P_{dif}, the estimation using the mechanistic model was significantly more precise (e.g.: deltorphin II Oatp1b2-associated V_{max} was estimated at 82.6±23.3 pmol/mg/min with the mechanistic model and 56.1±39.2 pmol/mg/min with the two-step approach). While for fexofenadine – characterized by a medium P_{dif} in rat hepatocytes (2.08±0.67 µl/mg/min) – the difference in K_m estimation by the two methods was larger: 271±35 µM and 27.2±29.2 µM for the mechanistic model and the two-step approach respectively. In addition the estimate obtained from the two-step approach was associated with a high uncertainty (CV=107%).

Discussion

The quantitative assessment of active transport requires careful evaluation of the experimental procedure as well as an appropriate mathematical model to quantify and integrate both passive and active processes. Therefore, the conditions for *in vitro* uptake studies were optimized and data were analyzed with a mechanistic model to quantify in one single step the passive and active processes derived from the *in vitro* cellular uptake assays. In addition, this mechanistic model includes disappearance of compound from the incubation medium, bidirectional passive diffusion and non-specific binding.

Optimization of experimental conditions for the *in vitro* assessment of active drug uptake.

In cellular uptake assays non-specific binding often leads to high apparent intracellular concentrations, misleading the subsequent data analysis due to elevated background (Obach, 1996). This is especially critical for higher substrate concentrations and for compounds with higher lipophilicity. Therefore, experimental conditions, in particular the washing steps, were modified to reduce such non-specific binding. The optimization of the washing steps showed, that in particular the temperature of wash buffer influenced the efficiency of the washing. An increased efficiency was seen if wash buffer was used at 37ºC as compared to 4ºC. The potential of leakage of intracellular compound during the washing at elevated temperature was found to be similar at either temperature of the washing buffer used (Figure 2). In any case, the washing should be fast to avoid significant levels of compound leakage. Remaining non-specifically bound material was taken into account during the kinetic analysis of transport data.

Different methods are used to assess passive diffusion independently from active transport in cellular uptake assays. Cell lines over-expressing individual transporters have in theory the

advantage that any passive processes, such as non-specific binding and passive diffusion, can be assessed by using the parental cell lines in parallel uptake studies. For primary cells, such as hepatocytes, the passive processes are more difficult to assess. In this respect control incubations at 4°C are often performed to assess passive diffusion (Komai et al., 1992; Ismair et al., 2001; Shimada et al., 2003; Lancon et al., 2004; Treiber et al., 2004; Ho et al., 2006). For many transporter model substrates, such as taurocholate and estrone-3-sulfate which have negligible passive diffusion, this approach is appropriate. However, for many other, more lipophilic compounds characterized by potentially higher passive permeabilities, this approach is questionable. Thus, for such compounds the passive diffusion was found to be considerably lower at 4°C as compared to 37°C in parent cell lines and artificial PAMPA membranes (Figure 3 and 4B), indicating that such conditions would not be appropriate as control incubation for some compounds. In this study, P_{dif} values were obtained for three transporter substrates CCK8, deltorphin II and fexofenadine in both, the control CHOneo cells – where only P_{dif} was estimated – and CHO-Oatp cells – where P_{dif} and active processes were estimated simultaneously with the proposed mechanistic model (Figure 4A).These values were not statistically different, but because of high variability for the low P_{dif} values (CCK8-deltorphin II) the study was underpowered to detect a difference. However both estimations yielded medium P_{dif} for fexofenadine and extremely low values for CCK8 and deltorphin II. For rat hepatocytes incubated at 37°C, the P_{dif} was assessed by the same approach and was different from the P_{dif} measured at 4°C (Figure 4B). Therefore, in all following *in vitro* experiments, P_{dif} was assessed together with V_{max} and K_m in the same experiment, without using control CHO control cells or rat hepatocytes at 4°C.

Analysis of data from *in vitro* transport experiments.

Often *in vitro* uptake transport data are evaluated by a step-wise approach. The initial transport rates are determined, often in single time point experiments, followed by a secondary plot of these rates versus substrate concentrations. Kinetic parameters (V_{max}, K_m) and P_{dif} are then calculated by regression analysis utilizing equation 2 (Komai et al., 1992; Ismair et al., 2001; Treiber et al., 2007; Webborn et al., 2007). This approach assumes linear conditions for the determination of initial uptake rates. It proved to produce reliable parameters for compounds for which P_{dif} and non-specific binding were negligible (compound 3 in Figure 6; CCK8 and deltorphin II in Table 1). However, for compounds with higher permeability the assumption of linearity of the initial uptake is not valid because of the physiological bidirectionality of P_{dif}. The usual assumption underlying this approximation is, that within the very short time of an uptake experiment (<2 min), a concentration gradient driving the export of the drug through passive diffusion is negligible. However, in the experimental set-up used in this study where the incubation medium volume was about 150-fold higher than the intracellular volume (V_{me}=150 µl; $V_{intracell}$~1 µl), the drug incubated rapidly reached very high intracellular concentrations relative to extracellular concentrations, so that the passive diffusion of the compound back into the extracellular medium becomes significant and leads to non-linear uptake rates. For example pitavastatin incubated in rat hepatocytes showed intracellular concentrations of 9 µM after 30 seconds incubation for a C_{me} of 0.6 µM, while for fexofenadine the intracellular concentration was 3.5 µM after 30 seconds incubation for a C_{me} of 2 µM. This rapid intracellular accumulation of some substrates leads to a non-linear uptake rate as seen for fexofenadine, pitavastatin and compound B (Figure 7G, H) which warrants the kinetic determination of the uptake with multiple time points. For low permeability compounds such as the classical model substrates used in uptake transport studies, eg. estrone-3-sulfate, taurocholate and also CCK8 (Figure 7A-C) such a non-linearity is not seen as uptake is then mainly driven by the active transport component.

Mechanistic two compartment model describing bidirectional passive permeability and active transport.

A mechanistic model able to incorporate non-linearities by addressing the underlying physiologic processes involved, is proposed in this paper. One main advantage of this model is the possibility to describe the time-course of the relevant passive and active physiological processes observed under the experimental conditions, including active transport, bidirectional passive diffusion, and adsorption to cells and supportive materials in one single step. In addition, the model accounts for the time-dependant disappearance of compound from the incubation medium, which was incorrectly considered stable in the classical approach. This mechanistic model allows analysis of the whole set of raw data in one step, without any prior data transformation. The model allowed to determine the kinetic parameters for compounds with many diverse properties (P_{dif} up to 15 µl/mg/min, non-specific binding, diverse K_m/V_{max}) with higher precision compared to the conventional step-wise approach.

The assessment from virtual data sets generated for eight compounds with different properties, indicated that the kinetic parameters calculated using the mechanistic model were always closer to the initial values and much more accurate and precise than with the two-step approach (Figure 6). The analysis of *in vitro* transport data for five diverse compounds, utilizing primary rat hepatocytes and CHO cells over-expressing Oatp/OATP transporters, clearly supported the advantages of the mechanistic model over the conventional two-step approach. For CCK8 and deltorphin II, which are selective substrates of Oatp1b2 (own data, (Ismair et al., 2001)), the mechanistic model yielded comparable K_m values in rat hepatocytes and in CHO-Oatp1b2 cells, whereas the two-step approach resulted in 2- to 3-fold different K_m values (Table 1). Most importantly, in all cases, the variation on K_m and V_{max} was significantly lower if the mechanistic model was used for data evaluation.

A similar mechanistic approach was recently published by Baker and Parton (2007). In contrast to the model proposed by these authors, where intra- and extra-cellular protein binding is modeled based on association and dissociation kinetics (k_{on} and k_{off} rates), a single parameter was chosen in the present study to describe adsorption to the cells and other non-specific binding, in order to reduce the number of parameters. The present *in vitro* experimental set up has been developed for the evaluation of uptake transport parameters only, and no protein was added in the incubation. In contrast to the study of Baker and Parton, the validity of the present model was demonstrated for several drugs, some of them being studied in three different cell types. The present study also used a different experimental *in vitro* approach. Plated cells, whether freshly isolated primary rat hepatocytes, or cell lines over-expressing different transporters, were used here rather than suspensions. This allows for the assessment of transport under the same experimental conditions and gives the possibility to reduce non-specific binding by multiple washing steps.

In addition to the evaluation of experimental data, the mechanistic model can be used to optimize the experimental design (i.e. optimal sampling times and medium concentrations) based on compound properties, such as solubility, lipophilicity and expected permeability. The analysis with the mechanistic model shows also one important limitation in the estimation of transport parameters when P_{dif} values increase beyond 15 µl/mg/min (Figure 5B and D) as shown for example for compound B. Furthermore the model allows to quantify the impact of the uncertainty associated with some parameters.

The mechanistic model was set-up for two compartments describing the situation in cellular uptake transport studies. Further refinement of the model will be required in the future to assess data from different *in vitro* assays. Thus, the analysis of *in vitro* transport data coming from cells seeded on filter inserts requires a third compartment as suggested by Sun and Pang (2008), Bentz et al., (2005) and Gonzalez-Alvarez et al.(2005).

In conclusion, the *in vitro* experimental protocol to assess uptake transport more quantitatively has been optimized in this study. Furthermore, the present mechanistic model proved to be a major improvement to the conventional two-step approach. It allows precise and accurate estimation of *in vitro* transport parameters from cellular uptake transport processes in one step, including bidirectional passive diffusion and non-specific binding. The analysis with the mechanistic model has also highlighted some limitations in the estimation of kinetic parameters *in vitro*. This quantitative evaluation of the kinetic transport parameters provides the basis for a solid PBPK modeling of active drug transport processes in connection to major parameters of drug metabolism aiming at a better prediction of overall hepatic drug elimination.

Acknowledgment

The authors thank Jean-Michel Scherrmann and Philippe Coassolo for advice and support in many helpful discussions throughout this project and Neil Parrott for carefully reading the manuscript.

References

Avdeef A, Strafford M, Block E, Balogh MP, Chambliss W and Khan I (2001) Drug absorption in vitro model: filter-immobilized artificial membranes. 2. Studies of the permeability properties of lactones in Piper methysticum Forst. *Eur J Pharm Sci* **14:**271-280.

Baker M and Parton T (2007) Kinetic determinants of hepatic clearance: Plasma protein binding and hepatic uptake. *Xenobiotica* **37:**1110-1134.

Bentz J, Tran TT, Polli JW, Ayrton A and Ellens H (2005) The steady-state Michaelis-Menten analysis of P-glycoprotein mediated transport through a confluent cell monolayer cannot predict the correct Michaelis constant Km. *Pharm Res* **22:**1667-1677.

Blanchard N, Richert L, Notter B, Delobel F, David P, Coassolo P and Lave T (2004) Impact of serum on clearance predictions obtained from suspensions and primary cultures of rat hepatocytes. *Eur J Pharm Sci* **23:**189-199.

Boelsterli UA, Bouis P, Brouillard JF and Donatsch P (1988) In vitro toxicity assessment of cyclosporin A and its analogs in a primary rat hepatocyte culture model. *Toxicol Appl Pharmacol* **96:**212-221.

Brosnan JT and Qian D (1994) Endotoxin-induced increase in liver mass and hepatocyte volume. *Biochem Soc Trans* **22:**529-532.

Chandra P and Brouwer KL (2004) The complexities of hepatic drug transport: current knowledge and emerging concepts. *Pharm Res* **21:**719-735.

Cvetkovic M, Leake B, Fromm MF, Wilkinson GR and Kim RB (1999) OATP and P-glycoprotein transporters mediate the cellular uptake and excretion of fexofenadine. *Drug Metab Dispos* **27:**866-871.

Ekins S, Ecker GF, Chiba P and Swaan PW (2007) Future directions for drug transporter modelling. *Xenobiotica* **37:**1152-1170.

Fischer H, Kansy M, Avdeef A and Senner F (2007) Permeation of permanently positive charged molecules through artificial membranes--influence of physico-chemical properties. *Eur J Pharm Sci* **31:**32-42.

Frezard F and Garnier-Suillerot A (1998) Permeability of lipid bilayer to anthracycline derivatives. Role of the bilayer composition and of the temperature. *Biochim Biophys Acta* **1389:**13-22.

Gonzalez-Alvarez I, Fernandez-Teruel C, Garrigues TM, Casabo VG, Ruiz-Garcia A and Bermejo M (2005) Kinetic modelling of passive transport and active efflux of a fluoroquinolone across Caco-2 cells using a compartmental approach in NONMEM. *Xenobiotica* **35:**1067-1088.

Hallifax D and Houston JB (2006) Uptake and Intracellular Binding of Lipophilic Amine Drugs by Isolated Rat Hepatocytes and Implications for Prediction of in Vivo Metabolic Clearance. *Drug Metab Dispos* **34:**1829-1836.

Hirano M, Maeda K, Shitara Y and Sugiyama Y (2004) Contribution of OATP2 (OATP1B1) and OATP8 (OATP1B3) to the hepatic uptake of pitavastatin in humans. *J Pharmacol Exp Ther* **311:**139-146.

Hirano M, Maeda K, Shitara Y and Sugiyama Y (2006) Drug-drug interaction between pitavastatin and various drugs via oatp1b1. *Drug Metab Dispos* **34:**1229-1236.

Ho RH, Tirona RG, Leake BF, Glaeser H, Lee W, Lemke CJ, Wang Y and Kim RB (2006) Drug and bile acid transporters in rosuvastatin hepatic uptake: function, expression, and pharmacogenetics. *Gastroenterology* **130:**1793-1806.

Ishiguro N, Maeda K, Kishimoto W, Saito A, Harada A, Ebner T, Roth W, Igarashi T and Sugiyama Y (2006) Predominant contribution of OATP1B3 to the hepatic uptake of telmisartan, an angiotensin II receptor antagonist, in humans. *Drug Metab Dispos* **34:**1109-1115.

Ismair MG, Stieger B, Cattori V, Hagenbuch B, Fried M, Meier PJ and Kullak-Ublick GA (2001) Hepatic uptake of cholecystokinin octapeptide by organic anion-transporting polypeptides OATP4 and OATP8 of rat and human liver. *Gastroenterology* **121:**1185-1190.

Komai T, Shigehara E, Tokui T, Koga T, Ishigami M, Kuroiwa C and Horiuchi S (1992) Carrier-mediated uptake of pravastatin by rat hepatocytes in primary culture. *Biochem Pharmacol* **43:**667-670.

Kopplow K, Letschert K, Konig J, Walter B and Keppler D (2005) Human hepatobiliary transport of organic anions analyzed by quadruple-transfected cells. *Mol Pharmacol* **68:**1031-1038.

Lancon A, Delma D, Osman H, Thenot JP, Jannin B and Latruffe N (2004) Human hepatic cell uptake of resveratrol: involvement of both passive diffusion and carrier-mediated process. *Biochem Biophys Res Commun* **316:**1132-1137.

Lindberg, V. (1997). Uncertainties Error Propagation Graphing & Vernier Caliper: A reference manual for University Physics Laboratories, Rochester Institute of Technology.

Liu L and Pang KS (2006) An integrated approach to model hepatic drug clearance. *Eur J Pharm Sci* **29:**215-230.

Luttringer O, Theil FP, Lave T, Wernli-Kuratli K, Guentert TW and de Saizieu A (2002) Influence of isolation procedure, extracellular matrix and dexamethasone on the regulation of membrane transporters gene expression in rat hepatocytes. *Biochem Pharmacol* **64:**1637-1650.

Neuhoff S, Ungell AL, Zamora I and Artursson P (2005) pH-Dependent passive and active transport of acidic drugs across Caco-2 cell monolayers. *Eur J Pharm Sci* **25:**211-220.

Noe J, Portmann R, Brun ME and Funk C (2007) Substrate Dependent Drug-Drug Interactions between Gemfibrozil, Fluvastatin and Other Oatp Substrates on Oatp1b1, Oatp2b1 and Oatp1b3. *Drug Metab Dispos* **35:**1308-1314.

Obach RS (1996) The importance of nonspecific binding in in vitro matrices, its impact on enzyme kinetic studies of drug metabolism reactions, and implications for in vitro-in vivo correlations. *Drug Metab Dispos* **24:**1047-1049.

Parker AJ and Houston JB (2008) Rate limiting steps in hepatic drug clearance: comparison of hepatocellular uptake and metabolism with microsomal metabolism of saquinavir, nelfinavir and ritonavir. *Drug Metab Dispos*.

Petzinger-Ernst G-J (2006) Drug transporters in pharmacokinetics. *Naunyn-Schmiedeberg's Archives of Pharmacology* **372:**465-475.

Poirier A, Funk C, Lave T and Noe J (2007) New strategies to address drug-drug interactions involving OATPs. *Curr Opin Drug Discov Devel* **10:**74-83.

Ratanasavanh D, Lamiable D, Biour M, Guedes Y, Gersberg M, Leutenegger E and Riche C (1996) Metabolism and toxicity of coumarin on cultured human, rat, mouse and rabbit hepatocytes. *Fundam Clin Pharmacol* **10:**504-510.

Reinoso RF, Telfer BA, Brennan BS and Rowland M (2001) Uptake of teicoplanin by isolated rat hepatocytes: comparison with in vivo hepatic distribution. *Drug Metab Dispos* **29:**453-459.

Ries J and Wienen W (2003) Serine proteases as targets for antithrombotic therapy. *Drugs of the future* **28:**355-370.

Sarkadi B, Attisano L, Grinstein S, Buchwald M and Rothstein A (1984) Volume regulation of Chinese hamster ovary cells in anisoosmotic media. *Biochim Biophys Acta* **774:**159-168.

Seglen PO (1979) Hepatocyte suspensions and cultures as tools in experimental carcinogenesis. *J Toxicol Environ Health* **5:**551-560.

Shimada S, Fujino H, Morikawa T, Moriyasu M and Kojima J (2003) Uptake mechanism of pitavastatin, a new inhibitor of HMG-CoA reductase, in rat hepatocytes. *Drug Metab Pharmacokinet* **18:**245-251.

Shitara Y, Hirano M, Adachi Y, Itoh T, Sato H and Sugiyama Y (2004) In vitro and in vivo correlation of the inhibitory effect of cyclosporin A on the transporter-mediated hepatic uptake of cerivastatin in rats. *Drug Metab Dispos* **32:**1468-1475.

Shitara Y, Horie T and Sugiyama Y (2006) Transporters as a determinant of drug clearance and tissue distribution. *Eur J Pharm Sci* **27:**425-446.

Shitara Y, Li AP, Kato Y, Lu C, Ito K, Itoh T and Sugiyama Y (2003) Function of uptake transporters for taurocholate and estradiol 17beta-D-glucuronide in cryopreserved human hepatocytes. *Drug Metab Pharmacokinet* **18:**33-41.

Treiber A, Schneiter R, Delahaye S and Clozel M (2004) Inhibition of organic anion transporting polypeptide-mediated hepatic uptake is the major determinant in the pharmacokinetic interaction between bosentan and cyclosporin A in the rat. *J Pharmacol Exp Ther* **308:**1121-1129.

Treiber A, Schneiter R, Hausler S and Stieger B (2007) Bosentan is a Substrate of Human OATP1B1 and OATP1B3: Inhibition of Hepatic Uptake as the Common Mechanism of its Interactions with Cyclosporin A, Rifampicin and Sildenafil. *Drug Metab Dispos* **35:**1400-1407.

van Montfoort JE, Hagenbuch B, Groothuis GM, Koepsell H, Meier PJ and Meijer DK (2003) Drug uptake systems in liver and kidney. *Curr Drug Metab* **4:**185-211.

Vickers SE, Stow MW and Warr JR (1993) Relationship between multidrug resistance, hypersensitivity to resistance modifiers and cell volume in Chinese hamster ovary cells. *Cell Biol Int* **17:**477-485.

Webborn PJ, Parker AJ, Denton RL and Riley RJ (2007) In vitro-in vivo extrapolation of hepatic clearance involving active uptake: Theoretical and experimental aspects. *Xenobiotica* **37:**1090-1109.

Yamashiro W, Maeda K, Hirouchi M, Adachi Y, Hu Z and Sugiyama Y (2006) Involvement of transporters in the hepatic uptake and biliary excretion of valsartan, a selective antagonist of the Angiotensin ii at1-receptor, in humans. *Drug Metab Dispos* **34:**1247-1254.

Legends for figures

Figure 1.

Schematic presentation of the cell-based uptake assay by two inter-connected compartments corresponding to the incubation medium (compound concentration C_{me}) and intracellular space of all cells in one well (compound concentration $C_{intracell}$). P_{dif}, V_{max} and K_m represent passive diffusion, Michaelis-Menten maximum transport rate and affinity constant, respectively.

Figure 2.

Post-incubation time profile of the intracellular concentration of deltorphin II (5 µM) for different conditions of the first wash step. All cells were incubated under the same conditions (37°C incubation) and uptake was stopped with ice-cold buffer. The first wash solution was left at a temperature of 37ºC (close symbols) or 4ºC (open symbols) on the CHO parental cells (circles) and on CHO-Oatp1b2 overexpressing cells (squares).

Figure 3.

Effect of incubation temperature (37ºC or 4ºC) on passive diffusion in CHO parental cells (P_{dif} in µl/mg/min, left axis) and permeability in PAMPA (Pe $x10^{-6}$ cm/s, right axis) for six compounds. Quantitative P_{dif} and Pe increase at 37ºC incubation compared to 4ºC is indicated by a factor above each couple of bars. In CHO parental cells, estrone-3-sulfate, taurocholate, fexofenadine, fluvastatin and propranolol were incubated at 4 to 6 different concentrations C_{me} respectively from 3 to 100 µM, from 1 to 50 µM, from 2 to 750 µM, from 1 µM to 50 µM, from 2 to 50 µM all for 0.5, 1, 1.5 and 5 min. Properties compound A was incubated at 5 µM at 6 different time points under 5 min. P_{dif} was estimated with the mechanistic model using equation 4. The asterisks represent a statistically significant difference of the means shown by Student's t-test (* $p<0.05$, ** $p<0.01$).

Figure 4.

Comparison of passive diffusion (P_{dif} in µl/min/mg on left axis, in µl/min/10^6 cells on the right axis) in CHO Oatp overexpressing cells and control parent cells (A) and in rat hepatocytes incubated at 37ºC and 4ºC (B). Fexofenadine was tested in CHO-Oatp1a1 cells, and deltorphin II and CCK8 in CHO-Oatp1b2 cells (A). In CHO cells and rat hepatocytes, fexofenadine, deltorphin II and CCK8 were incubated at 6 or 7 different concentrations respectively from 2 to 600 µM, from 1 to 500 µM, from 1 to 300 µM all for 0.5, 1 and 1.5 min. P_{dif} was estimated with the mechanistic model using equation 4 for CHOneo cells and rat hepatocytes incubated 4ºC and equation 3 for CHO-Oatp overexpressing cells and rat hepatocytes incubated 37ºC. For CCK8 and deltorphin II in CHO cells the extremely low observed P_{dif} values were respectively 0.007±0.119 and 0.036±0.051 µl/min/mg in overexpressed cells and 0.013±0.060 and 0.085±0.051 µl/min/mg in parental cells. The asterisks represent a statistically significant difference of the means shown by Student's t-test (*$p<0.05$, ** $p<0.01$).

Figure 5.

Simulation of time profiles of intracellular concentrations when P_{dif} is low and K_m decreases (A), P_{dif} is high and K_m decreases (B), P_{dif} is low and V_{max} increases (C), P_{dif} is high and V_{max} increases (D) and when K_m and V_{max} are fixed and P_{dif} increases (E).

Figure 6.

Differences in the evaluation of K_m, V_{max} and P_{dif} for a diverse set of virtual compounds (numerated 1 to 8) when either the mechanistic model or the classical two-step approach were used for data analysis. Six datasets per compound were randomly generated (n=6 virtual *in vitro* experiments) as indicated in Materials and Methods. Virtual compound properties were: **1.**K_m = 32 µM - V_{max} = 350 pmol/mg/min - P_{dif} = 1.20 µl/mg/min - $V_{intracell}$ = 1 µl - incubation time points = 30s, 60s, 90s - no binding. **2.**Compound 1 with incubation time points = 15s, 45s, 120s. **3.**Compound 1 with **P_{dif} negligible** (= 0.01 µl/mg/min). **4.**Compound 1 with **high**

P_{dif} (= 14 µl/mg/min) and V_{max} = 550 pmol/mg/min. **5.**Compound 1 with non-specific binding **(f_b=0.4) 6.**Compound 1 with non-specific binding **(f_b=0.15) 7.**K_m = 150 µM - V_{max} = 2000 pmol/mg/min - P_{dif} = 3.00 µl/mg/min - $V_{intracell}$ = 1 µl - incubation time points = 30s, 60s, 90s - no binding. **8.High P_{dif} + binding**: K_m = 32 µM - V_{max} = 550 pmol/mg/min - P_{dif} = 8.00 µl/mg/min - $V_{intracell}$ = 1 µl - incubation time points = 15s, 60s, 90s - f_b=0.15. Estimation of f_b by the mechanistic model was 0.382±0.105 for compound 5, 0.113±0.072 for compound 6, 0.171±0.139 for compound 8. The asterisks represent a statistically significant difference of the CV% shown by Student's t-test (* $p<0.05$, ** $p<0.01$, *** $p<0.001$).

Figure 7.

Incubation time profiles of the uptake of CCK8 in rat hepatocytes (A), CHO-Oatp1b2 cells (B) and CHO-OATP1B3 cells (C), deltorphin II in rat hepatocytes (D) and CHO-Oatp1b2 cells (E), fexofenadine in rat hepatocytes (F) and CHO-Oatp1b2 cells (G), pitavastatin calcium in rat hepatocytes (H) and napsagatran in rat hepatocytes (I). In rat hepatocytes incubated at 37ºC, napsagatran, pitavastatin, fexofenadine, deltorphin II and CCK8 were incubated at 6 or 7 different concentrations respectively from 15 to 500 µM, 0.6 to 600 µM, 2 to 750 µM, from 1 to 200 µM, from 1 to 300 µM all for 0.5, 1 and 1.5 min. In CHO cells incubated at 37ºC, fexofenadine, deltorphin II and CCK8 were incubated at 6 or 7 different concentrations respectively from 2 to 600 µM, from 1 to 500 µM, from 1 to 300 µM all for 0.5, 1 and 1.5 min. Incubation medium concentrations (C_{me}) and fitted lines of the mechanistic model are indicated below the graphs. Mean parameters over triplicate experiments are found in Table 1.

Table 1. Effect of the kinetic analysis method used for evaluation of K_m, V_{max} and P_{dif} from *in vitro* experiment data of CCK8, deltorphin II, fexofenadine, pitavastatin and napsagatran: mechanistic model compared to conventional two-step approach. In rat hepatocytes incubated at 37ºC, napsagatran, pitavastatin, fexofenadine, deltorphin II and CCK8 were incubated at 6 or 7 different concentrations respectively from 15 to 500 µM, 0.6 to 600 µM, 2 to 750 µM, from 1 to 200 µM, from 1 to 300 µM all for 0.5, 1 and 1.5 min. In CHO cells incubated at 37ºC, fexofenadine, deltorphin II and CCK8 were incubated at 6 or 7 different concentrations respectively from 2 to 600 µM, from 1 to 500 µM, from 1 to 300 µM all for 0.5, 1 and 1.5 min. Individual coefficients of variation (CV) are presented in italic between brackets next to the values. Mean CV represents the average of each individual CV in one column.

	K_m (µM)		**V_{max} (pmol/mg/min)**		**P_{dif} (µl/mg/min)**	
	mechanistic model	two-step approach	mechanistic model	two-step approach	mechanistic model	two-step approach
CCK8						
Rat hepatocytes	20.1±2.5 *(12.4%)*	22.4±12.0 *(53.6%)*	421±34 *(8.1%)*	440±121 *(27.5%)*	0.805±0.215 *(26.7%)*	0.104±0.453 *(436%)*
CHO-Oatp1b2	13.9±2.4 *(17.3%)*	8.6±5.8 # *(67.4%)*	73.0±9.9 *(13.6%)*	78.9±23.2 *(29.4%)*	0.029±0.054 *(186%)*	0.007±0.119 *(1700%)*
CHO-OATP1B3	15.2±2.2 *(14.5%)*	22.1±18.5 *(83.7%)*	238±25 *(10.5%)*	278±117 *(42.1%)*	0.311±0.128 *(41.1%)*	0.076±0.369 *(486%)*
Deltorphin II						
Rat hepatocytes	150±99 *(66.0%)*	130±167 *(128%)*	190±118 *(62.0%)*	232±318 *(137%)*	0.210±0.211 *(100%)*	0±0.400
CHO-Oatp1b2	118±36 *(30.5%)*	64.9±80.7 *(124%)*	82.6±23.3 *(28.2%)*	56.1±39.2 *(70.0%)*	0.030±0.042 *(139%)*	0.036±0.051 *(142%)*
Fexofenadine						
Rat hepatocytes	271±35 *(12.9%)*	27.2±29.2 *(107%)*	3162±274 *(8.7%)*	391±146 *(37.3%)*	2.08±0.67 *(31.7%)*	3.26±0.26 *(8.0%)*
CHO-Oatp1a1	51.0±19.0 *(37.3%)*	12.3±37.9 *(308%)*	580±134 *(23.0%)*	144±110 *(96.5%)*	6.40±1.19 *(18.7%)*	3.14±0.24 *(7.6%)*
Pitavastatin [a]						
Rat hepatocytes	71.7±6.9 *(9.6%)*	62.7±36.0 *(57.4%)*	8419±897 *(10.6%)*	5876±1728*(29.4%)*	0.909±1.043 *(115%)*	3.23±2.30 *(71.2%)*
Napsagatran						
Rat hepatocytes	88.4±8.1 *(9.2%)*	31.3±32.3 *(103%)*	384±19 *(5.0%)*	337±180 *(53.4%)*	0	0
MEAN CV	***23.3%***	***115%*****	***18.9%***	***58.1%******	***82.3%***	***407%***

The asterisks represent a statistically significant difference of the CV between the two approaches shown by Student's t-test (** $p<0.01$, *** $p<0.001$). The hash sign represents a statistically significant difference between K_m of CHO-Oatp1b2 and K_m of rat hepatocytes shown by Student's t-test (# $p<0.05$).

[a] mechanistic model estimated fraction bound to 0.21 ± 0.10 for pitavastatin (zero for the four other compounds)

Figure 1

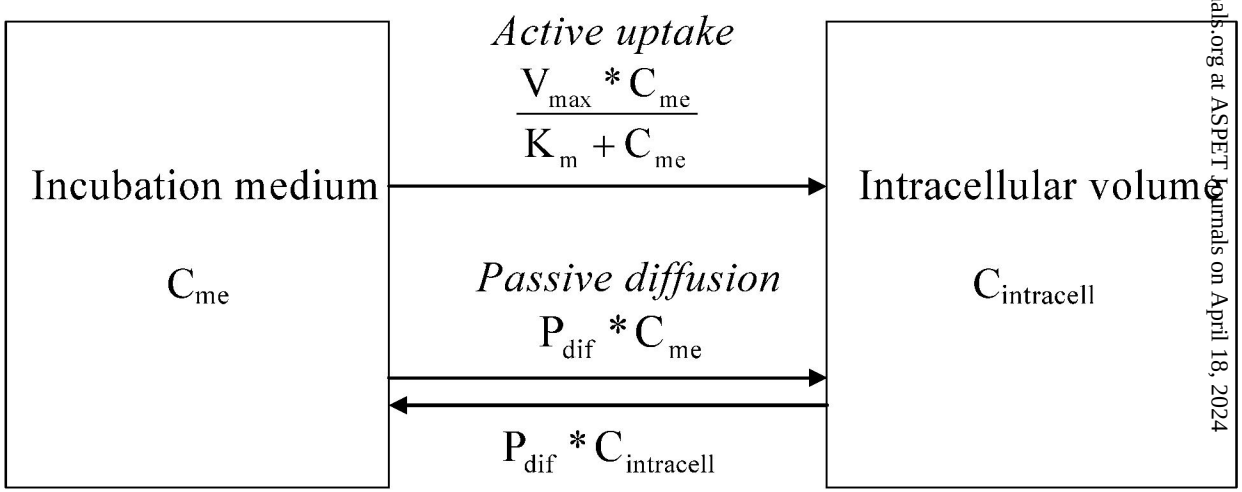

Figure 2

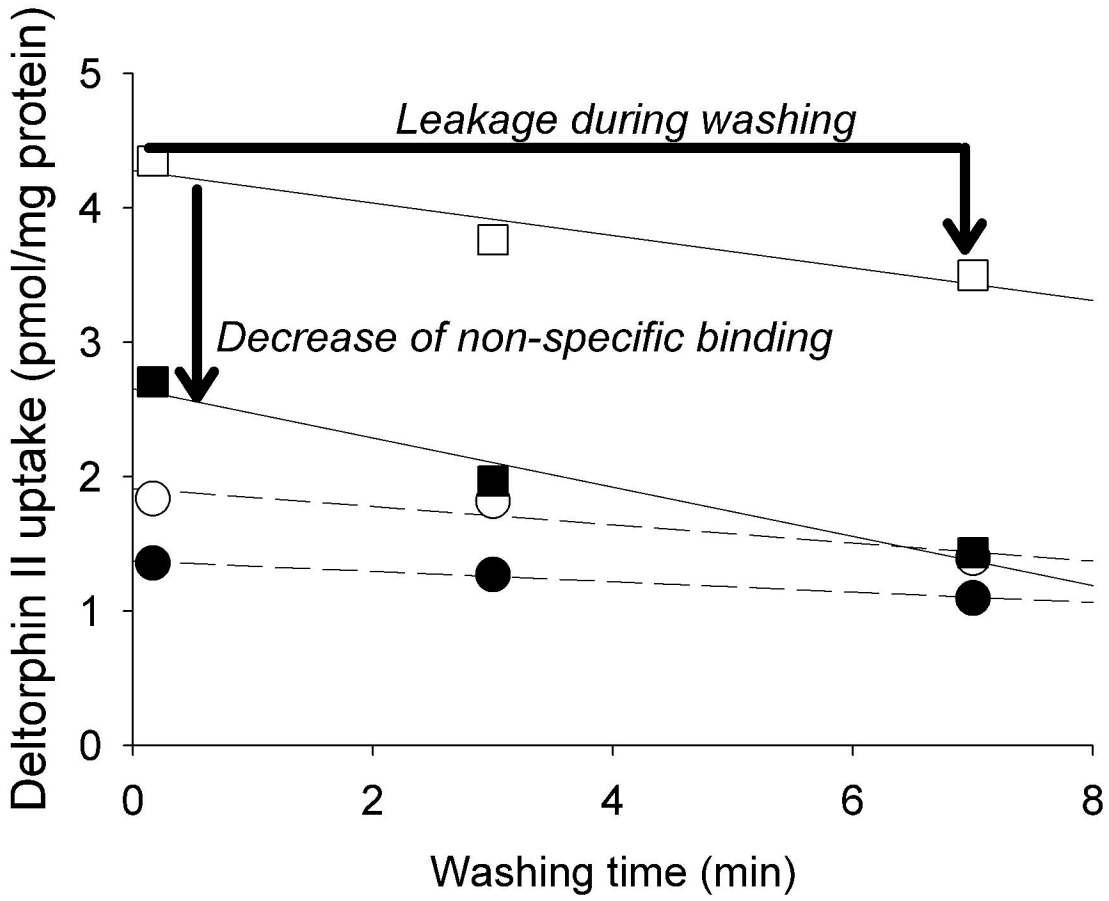

DMD Fast Forward. Published on September 22, 2008 as DOI: 10.1124/dmd.108.020750
This article has not been copyedited and formatted. The final version may differ from this version.

Figure 3

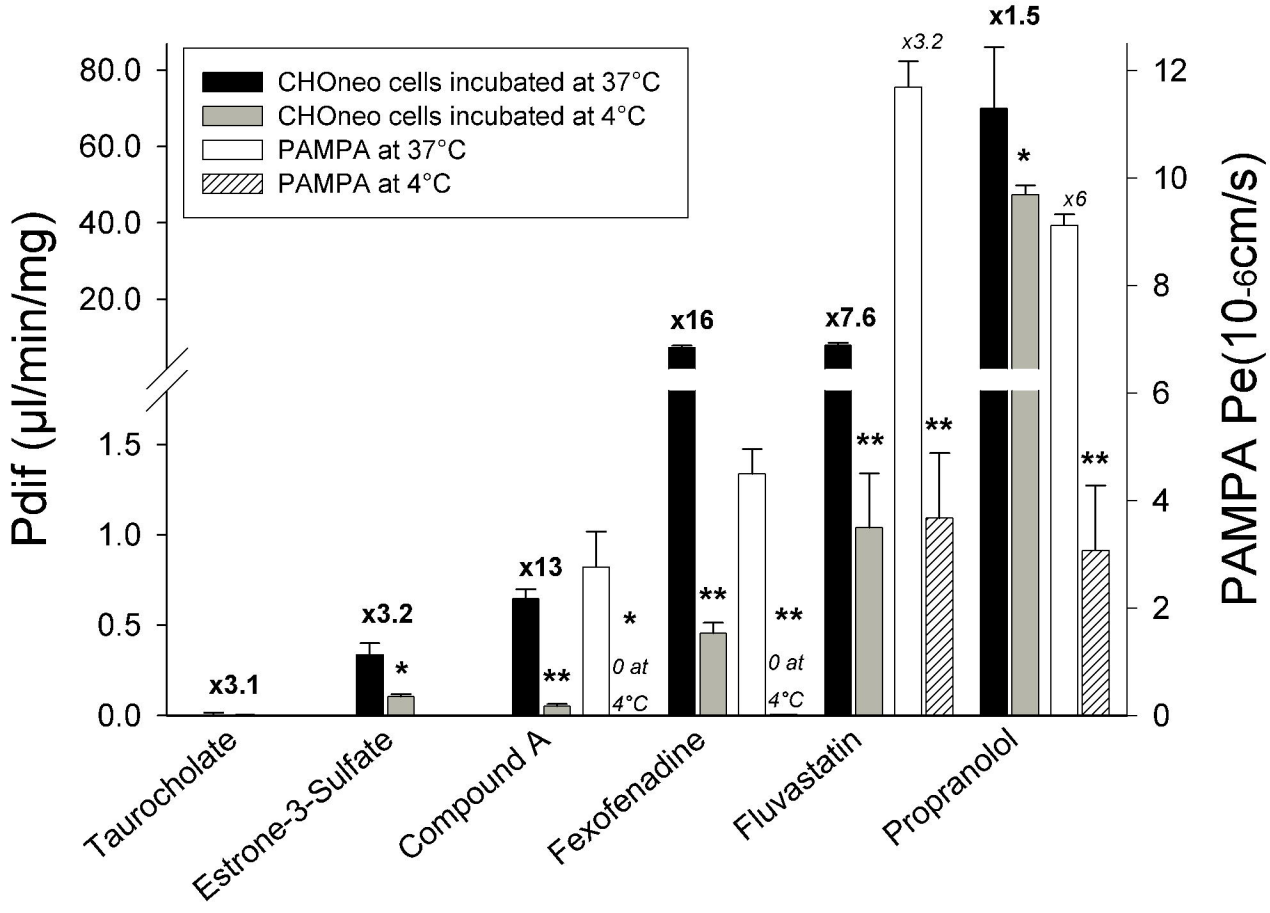

Figure 4

DMD Fast Forward. Published on September 22, 2008 as DOI: 10.1124/dmd.108.020750
This article has not been copyedited and formatted. The final version may differ from this version.

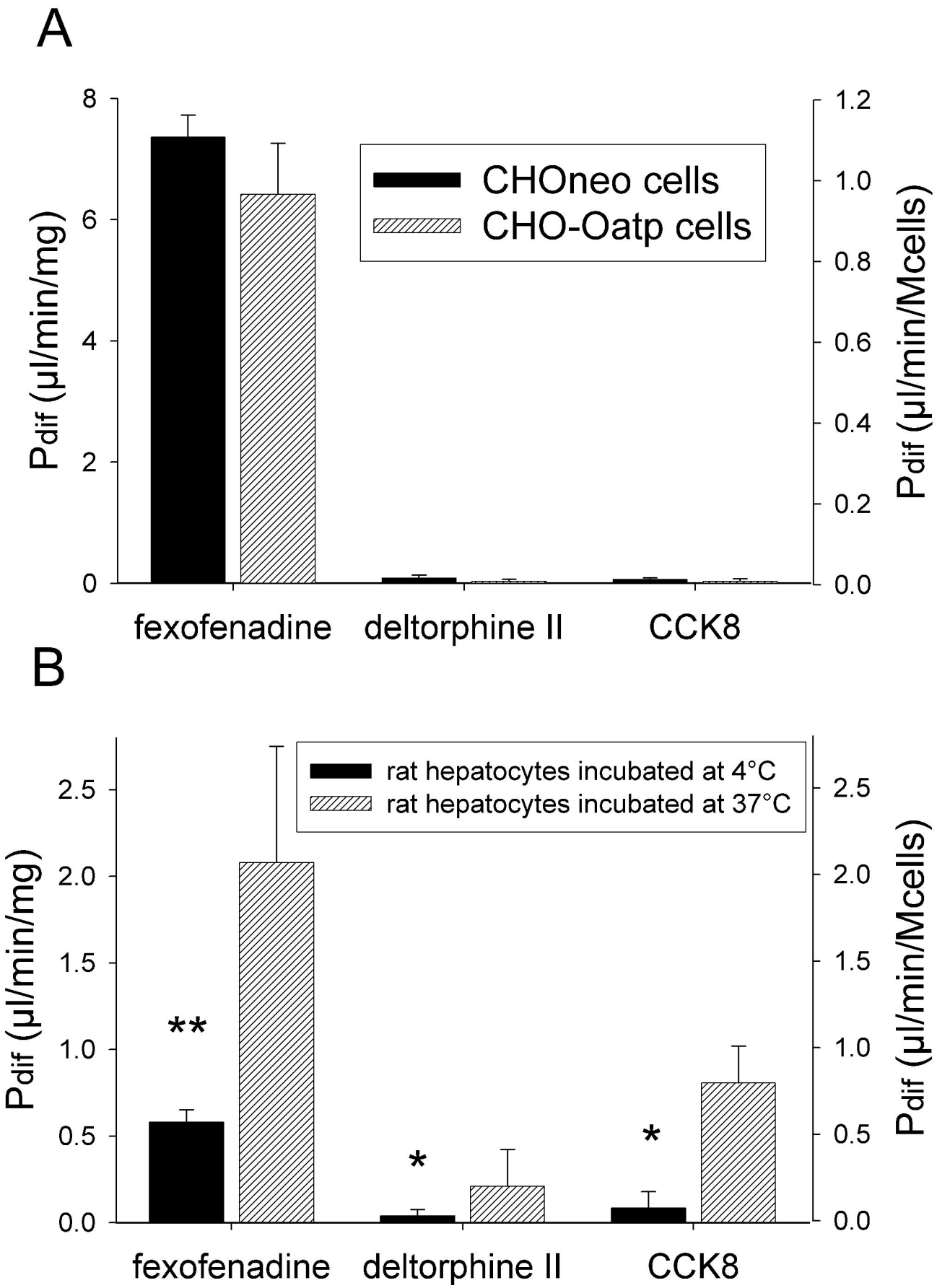

DMD Fast Forward. Published on September 22, 2008 as DOI: 10.1124/dmd.108.020750
This article has not been copyedited and formatted. The final version may differ from this version.

Figure 5

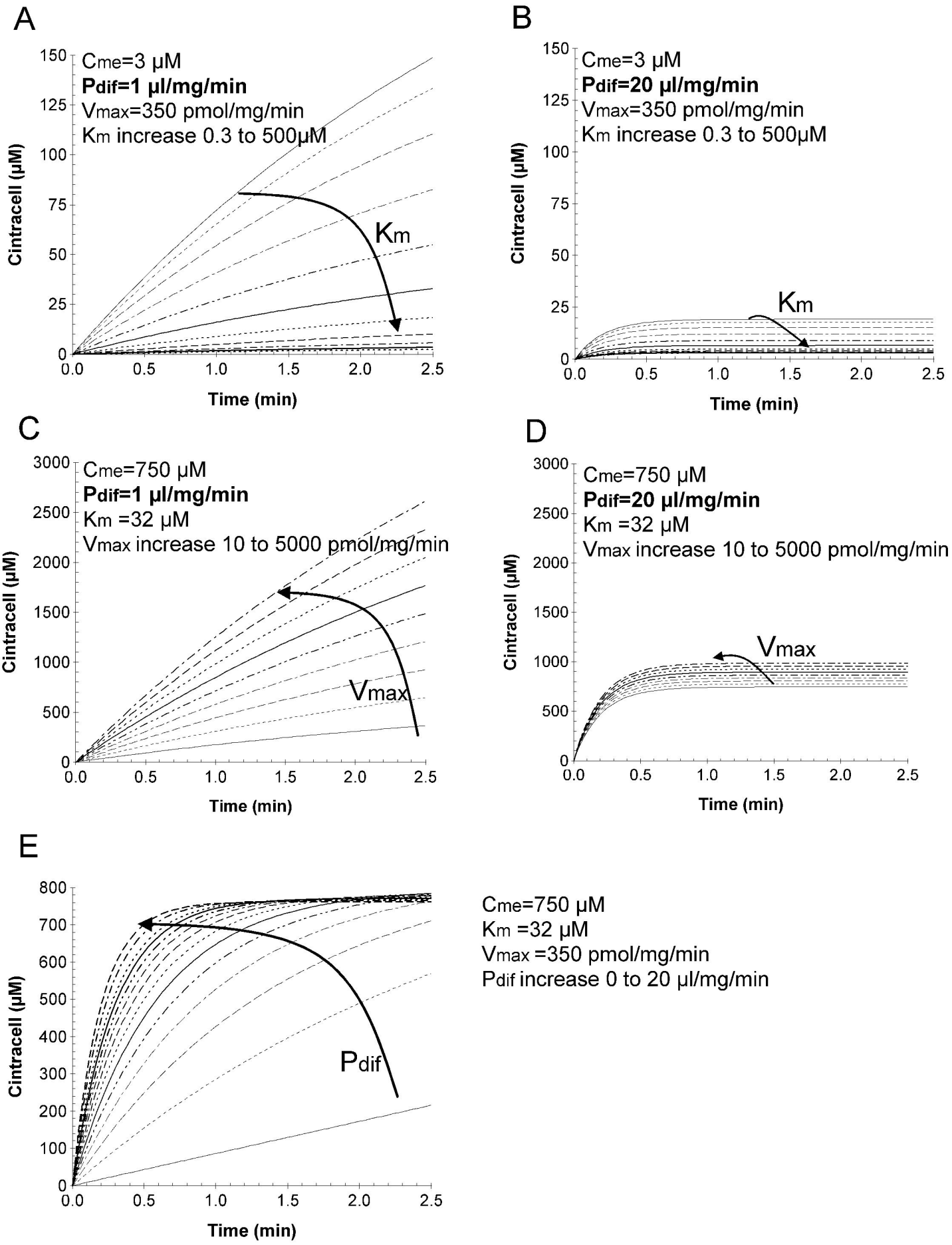

DMD Fast Forward. Published on September 22, 2008 as DOI: 10.1124/dmd.108.020750

Figure 6

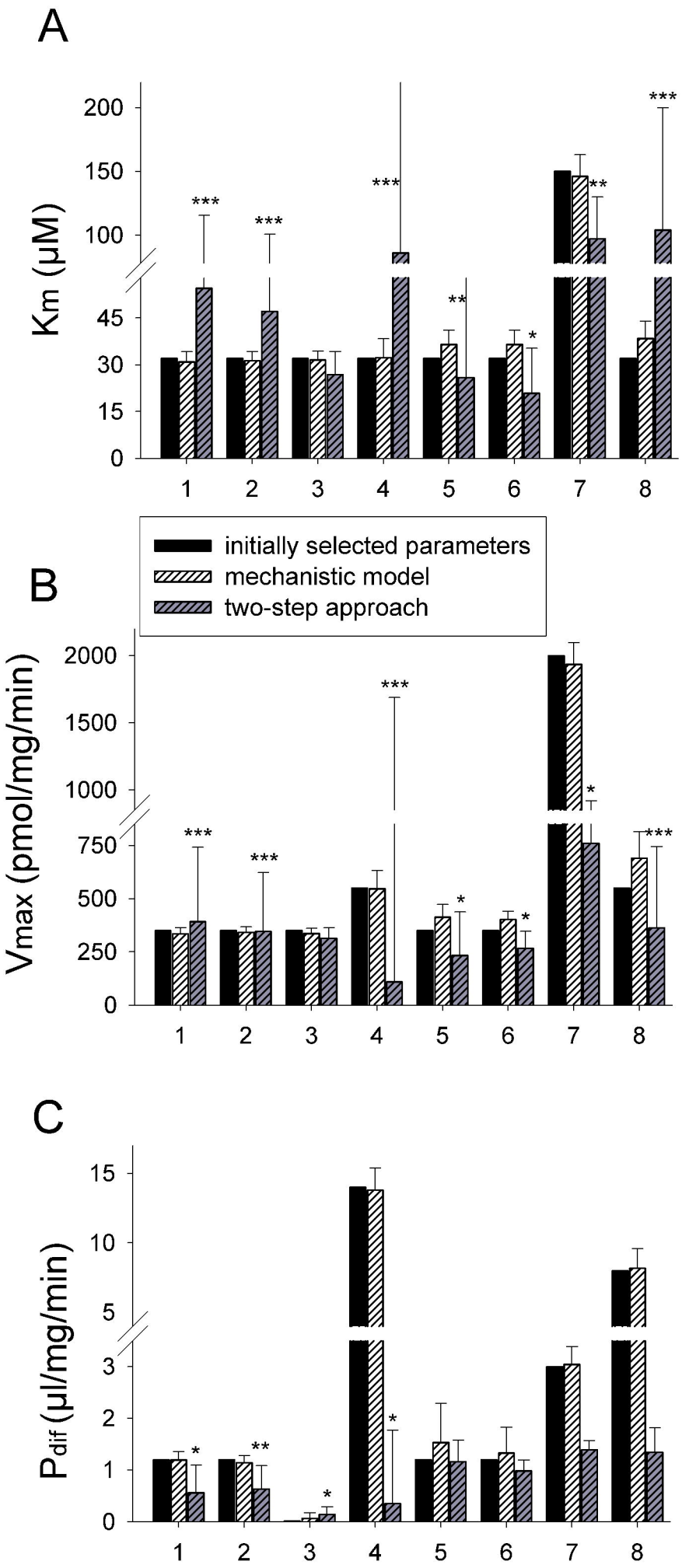

Figure 7